Hindawi
Mathematical Problems in Engineering
Volume 2022, Article ID 4578868, 18 pages
https://doi.org/10.1155/2022/4578868

Research Article

Multiobjective Model for Microgrids Integrating Electric Vehicles to Grid and Building Based on Interest Balance

Xiaolin Chu,[1] **Peng Wang**,[2] **and Dong Yang**[3]

[1]*School of Financial Technology, Shanghai Lixin University of Accounting and Finance, Shanghai 201209, China*
[2]*Science and Technology on Electromagnetic Scattering Laboratory, Shanghai 200438, China*
[3]*Glorious Sun School of Business and Management, Donghua University, Shanghai 200051, China*

Correspondence should be addressed to Dong Yang; yangdong@dhu.edu.cn

Received 5 November 2022; Revised 11 December 2022; Accepted 17 December 2022; Published 27 December 2022

Academic Editor: Yang Li

Microgrids allow energy exchange among multiple interconnected microgrids for greater energy efficiency and collective economic interest. However, in some cases, the benefit of some microgrids within the network may not be uncertain. In view of the increasing development of electric vehicles (EVs), a multiobjective model is proposed to improve the performance of microgrids by integrating electric vehicles-to-grid (V2G) and vehicles-to-building (V2B) based on global and individual benefit balance. Two reference models are built to verify the validity of the proposed method, and models are formulated as mixed integer linear programming formats solved by the weighting method. A set of parameters of microgrids are adopted to model the driver behaviors (e.g., available hours of EV), energy transactions (e.g., electricity), performance factor (e.g., emission factor), distributed energy (e.g., solar panel), and energy load of five commercial buildings (e.g., hotel) located in Shanghai. Simulation results demonstrate the effectiveness of the operation decision models in the energy management of microgrids under neutral, pro-economic, proenvironmental, and proenergy weighting scenarios. The case study results specify that the proposed method can achieve operational cost, CO_2 emission, and primary energy consumption reductions for each microgrid, with total benefits declining slightly.

1. Introduction

Global energy consumption has been continuously increasing due to population growth, economic development, and accelerated urbanization in recent years. As a larger proportion of energy consumption, electricity demand is expected to increase by almost 28% from 23,300 terawatt-hours (TWh) in 2020 to almost 30,000 TWh by 2030 [1]. To accommodate a reliable supply of power to customers, the power grid's infrastructure needs to be upgraded and expanded, which might lead to high capital investments and serious environmental pollution. To deal with these issues, the microgrid technology has been developed rapidly in recent years which consist of distributed energy sources (e.g., renewable energy resources, power generators, and storage system) and energy loads [2]. The microgrid can provide a good opportunity to effectively improve energy utilization and reduce environmental pollution and is expected to play a significant role in building smart cities in many countries [3–5].

The microgrid can be defined as an electricity bounded area of distributed network that aggregates locally distributed generation sources (e.g., solar power generation) along with energy storage devices (e.g., electric storage) and controllable loads (e.g., electricity load) so as to form a self-sufficient energy system [6]. Following the increase in electricity demand, the energy efficiency of a microgrid may be restricted due to the limited capacity of locally distributed generation sources in a bounded area. Based on the development of Internet technology, different microgrids can operate collaboratively to improve efficiency and reliability as well as economy by exchanging energy with each other, which is regarded as microgrids technology [7, 8]. In the past few

decades, extensive research has been tried to obtain energy efficient operation strategies for individual microgrid and microgrids.

As for an individual microgrid, existing works mainly focus on optimizing energy dispatch with the aim to maximize economic benefit [9, 10], environmental benefit, and reliability [11]. For example, due to the high energy utilization efficiency of combined cooling, heating, and power (CCHP) systems, authors in [12] use a novel two-stage coordinated control approach to solve the CCHP microgrid energy management problem with the objective to minimize cost. In order to reduce operation costs, reduce gas emissions, and increase consumer satisfaction, the authors in [13] present a practical multiobjective dynamic optimal dispatch model incorporating energy storage and user experience. At the same time, in view of the increasing development of EVs, vehicle-to-grid (V2G) and vehicle-to-building (V2B) technologies are proposed to overcome fluctuations in the voltage and frequency caused by EVs' charging [14–16]. In V2G and V2B bidirectional communication, EVs can supply electricity to a power grid/building with the utilization of bidirectional converters under plugged-in EVs. The authors in [17] focus on balancing the interests between microgrids and EV battery swapping stations and propose a new bilevel optimal scheduling model under multistakeholder scenarios. Furthermore, the authors in [18] extend the mathematical model to coordinate flexible demand response and multiple renewable uncertainties. However, the interest conflict among microgrids is ignored.

Due to the economic performance and power generation reliability of microgrids, the collaborative operation among microgrids has recently drawn the attention of the researcher. The operation process of microgrids is more complex, as multiple renewable energy sources are complemented and multiple types of energy are exchanged [19]. Several efforts (e.g., framework development, modelling, and solution methods) are made to study microgrids in order to take full advantage of the services and benefits [20–22]. The authors in [23] study the energy sharing and trading on a novel spatiotemporal energy network through V2B and V2G interaction and evaluate the techno-economic-environmental potentials of the proposed energy network. Stochastic and robust optimization-based collaborative operation approaches for microgrids are formulated to derive the energy scheduling scheme, whose objective is to minimize the total microgrids' operation costs under uncertain factors [19, 24]. Multiobjective optimization dispatch for microgrids with EV charging is studied to achieve minimized operation cost, greenhouse gas emission reductions, and enhanced reliability of services [25]. These operation decision models mainly focus on maximizing collective benefits by aggregating all the entities into the overall microgrid system as one unit, while the benefit of individual microgrid is not considered.

However, the individual interest of each microgrid may be damaged if only the benefits of microgrids are focused. The conflicts of interests will lead to microgrids being disbanded when the microgrid's operators are heterogeneous (i.e., independent) and profit-driven entities. To address this problem, balancing the collective and individual economic benefits should be focused on obtaining a scheduling energy strategy to implement microgrids with coordinated operations [26, 27]. A mathematical decision framework is presented in [28] to research the transactive energy management of microgrids under the local energy transaction market. Furthermore, chance-constrained models using a transactive energy structure are proposed to manage energy exchange in microgrids considering uncertainty, and simulation results prove that microgrids can gain both collective and individual economic benefits based on the mechanism [29]. However, methods balancing global and local benefits of microgrids with multiple perspectives came from real-world problems are missing. And decision makers' preferences are less focused on the microgrid optimization problem.

To bridge these research gaps, we propose the multiobjective model for the microgrids integrating V2G and V2B based on interest balance to ensure individual microgrid's benefit. EVs can be utilized as dynamically configurable dispersed energy storages to balance the energy supply and demand in microgrids. The objectives of microgrids are to minimize collective cost (COST), carbon dioxide emission (CDE), and primary energy consumption (PEC) and ensure individual microgrid's benefit. Three multiobjective models are formulated to examine the performance of variation, and different weight combinations are assumed to represent the preference of decision maker. The first reference model focuses on minimizing collective interests under no energy exchange among microgrids, buildings, and charging station (CS). The second reference model is to achieve collaborative Internet in microgrids integrating V2G and V2B, when energy can freely exchange among microgrids, buildings, and charging stations. The proposed model aims to maximize both the global and local interests of microgrids integrating V2G and V2B. In the case study, four scenarios are investigated for the microgrids in Shanghai under different importance levels of operators. In summary, the contributions of this research lie in three aspects: (1) A multiobjective mathematical decision framework is proposed to balance interest among individual microgrids and is discussed with reference problems; (2) the weighting method is used to solve the multiobjective models, and the weighting scenarios are set according to the decision markers' preferences; and (3) multidimensional experiments are analyzed in the case study to illustrate the models' scalability.

The rest of the paper is structured as follows: Section 2 describes the technical roadmap and problem description; in Section 3, a multiobjective collaborative model is built to describe the energy sharing in the microgrids; in Section 4,reference decision models are proposed; in Section 5,the numerical results from the case studies for the presented multiobjective energy management system of microgrids under different weighting scenarios are reported; and in Section 6,several conclusions are drawn.

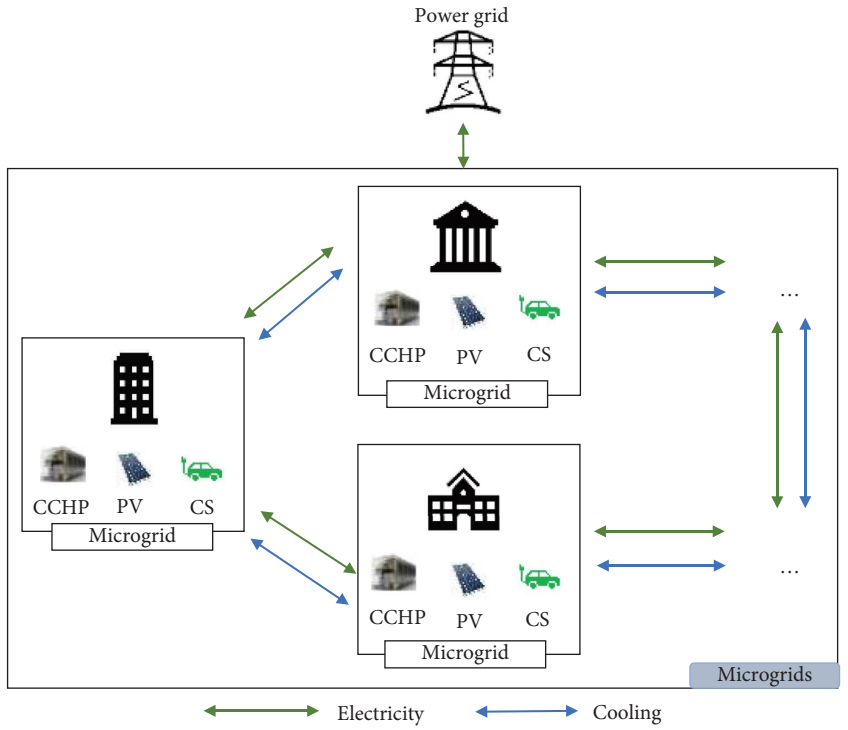

Figure 1: System layout of the proposed microgrids.

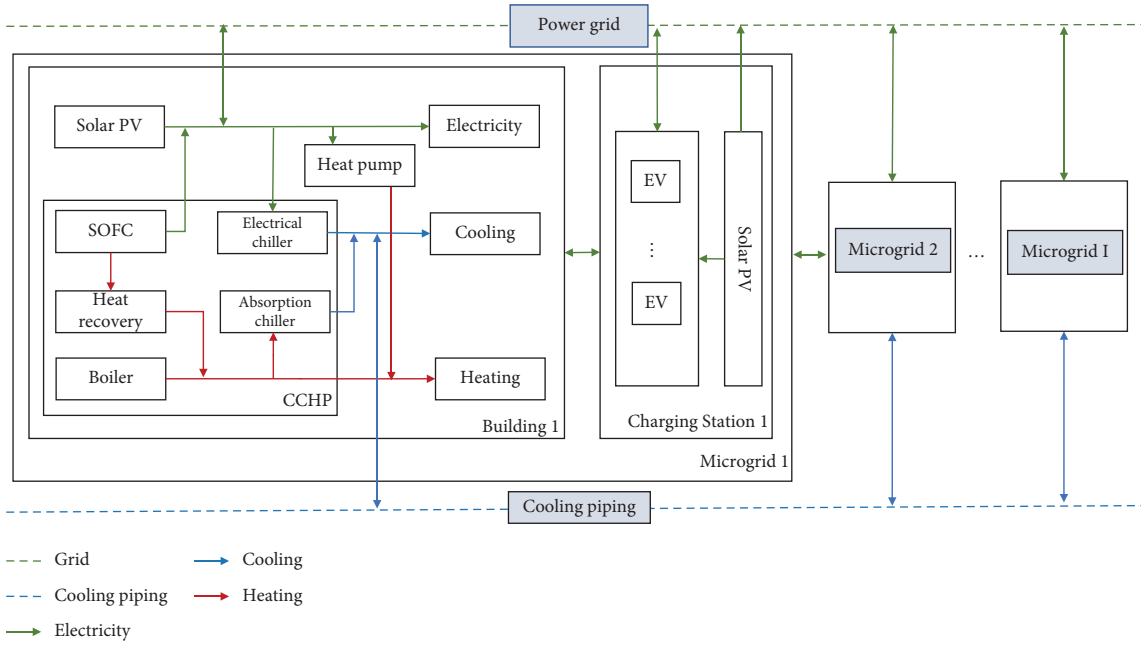

Figure 2: Overall schematic of the microgrids integrating V2G and V2B.

2. Problem Description

In this research study, a modelling framework is developed to study the energy management of microgrids. The layout of the proposed network is presented in Figure 1, and the overall system is comprised of the power grid and multiple microgrids. Each microgrid consists of an end user (e.g., building), a CCHP system, a photovoltaic (PV) panel, and a charging station. Electric vehicles arriving at charging stations are in two-way power exchange with the power grid and end users based on V2G and V2B technologies. In addition, localized cooling networks and microgrids are

established to enable electricity and cooling energy transfer within microgrids, which are depicted as solid lines with green and blue colors in Figure 1, respectively.

The specific layout of the proposed network is displayed in Figure 2, in which each microgrid can share and exchange electric and cooling energy with other microgrids through wires and pipes within the network, respectively. The microgrid is comprised of a power grid, building, and charging station. The building, as the end user, is equipped with a CCHP system and PV panels. Due to its higher efficiency and lower emissions, the stationary Solid Oxide Fuel Cell (SOFC) is deployed as the prime mover of a CCHP system to generate electricity. Heating energy can be produced by a recovery system, and fuel can be converted to heat by an auxiliary boiler to satisfy cooling and heating demand. The CS has the capacity to charge multiple EVs simultaneously, using power from its PV panels, power grid, building, and other microgrids. The microgrid network connects with the power grid and can be enabled to feed-in or purchase electricity from the grid.

The solid line in green color in Figure 2 represents electricity flow. The electric load of building in each microgrid is supplied by CCHP, utility grid, PV, CS, and other microgrids. The electric load of electric vehicles in each microgrid is satisfied by the utility grid, PV, buildings, and other microgrids. The solid lines with blue color and red color in Figure 2 show cooling flow and heating flow, respectively. The cooling load of the building in each microgrid is supplied by an absorption chiller in a CCHP system and in other microgrids by cooling piping. The heating load is satisfied by the heat pump and CCHP systems.

As shown in Figures 1 and 2, the goal of this study is to gain the optimal energy management strategy for the power grid, EVs, CCHP system, PV, and energy transaction with balancing global and individual benefits. By adopting the optimal strategy, the total proposed system and each microgrid economic, environmental, and energy performance can be maximized under the constraints of equipment features, buildings' loads, EVs characteristics (e.g., EV battery balance and energy demand). The COST, CDE, and PEC of the system optimal strategy are explored under the following four different weighting scenarios to provide a better view of performances in the case studies: neutral, proeconomic, proenvironmental, and proenergy.

3. Mathematic Model for the Microgrids

In this section, a mixed integer linear programming (MILP) model is formulated to minimize the economic cost, environmental pollution, and energy consumption by obtaining the optimal strategy for the microgrids integrating V2G and V2B technologies. The model is established from a systematic perspective by considering the interrelationships among the multiple microgrids. The notations of indexes, parameters, and variables applied in the model are displayed in Table 1. All the parameters and variables are nonnegative.

3.1. Constraints

3.1.1. Power Grid Capacity Constraints. The power purchased from the utility grid to building ($E_{i,t}^{gb}$) and charging station ($E_{i,t}^{\mathrm{gcs}}$) is restricted by the capacity of the utility grid ($\mathrm{CAP}^{\mathrm{grid}}$) as follows:

$$E_{i,t}^{gb} + E_{i,t}^{\mathrm{gcs}} \le \mathrm{CAP}^{\mathrm{grid}}, \forall i, \forall t, \tag{1}$$

where i and t are the number of microgrids and time, respectively.

3.1.2. Building Operation Decision Model

(a) *Electric Load Balance Constraints.* The electrical balance showed in equation (2) means that the electric supply should be equal to demand at time t for building in microgrid i. The electric supply on the left side consists of electricity generated by solar PV ($E_{i,t}^{\mathrm{bpv}}$), SOFC ($E_{i,t}^{fc}$), purchased from the grid ($E_{i,t}^{gb}$), the charging station ($E_{i,t}^{\mathrm{csb}}$) as well as other microgrids ($E_{j,i,t}^{\mathrm{mbtr}}$). The right (demand) side items of the electricity include electricity consumption by EC ($E_{i,t}^{ec}$) and HP ($E_{i,t}^{hp}$), electricity sold back to the utility grid ($E_{i,t}^{bg}$), building electric load ($E_{i,t}^{\mathrm{bel}}$), electricity transmitted to CS ($E_{i,t}^{\mathrm{bcs}}$), and other microgrids ($E_{i,j,t}^{\mathrm{mbtr}}$). The transmission loss of electric energy within the microgrids is considered by implementing the factor of L_{wire}.

$$\begin{aligned} E_{i,t}^{\mathrm{bpv}} + E_{i,t}^{fc} + E_{i,t}^{gb} + E_{i,t}^{\mathrm{csb}} + \sum_{j} E_{j,i,t}^{\mathrm{mbtr}} \times (1 - L_{\mathrm{wire}}) E_{i,t}^{ec} \\ + E_{i,t}^{hp} + E_{i,t}^{bg} + E_{i,t}^{\mathrm{bel}} + E_{i,t}^{\mathrm{bcs}} + \sum_{j} E_{i,j,t}^{\mathrm{mbtr}}, \forall i, t, j \ne i. \end{aligned} \tag{2}$$

(b) *Thermal Load Balance Constraints.* The heating balance is displayed in equation (3), where recovered heat ($Q_{i,t}^{re}$) from the SOFC power generation plus heating supply from the boiler ($Q_{i,t}^{bo}$) and heat pump ($Q_{i,t}^{hp}$) are used to satisfy the heating consumption of absorption chiller ($Q_{i,t}^{\mathrm{ach}}$) and the building heating load ($Q_{i,t}^{\mathrm{bhl}}$) in microgrid i. Similarly, the cooling balance showed in equation (4) means that the cooling energy supply should be equal to electric demand at time t for building in microgrid i. The left (supply) side of the cooling demand includes the cooling generated by absorption chiller ($Q_{i,t}^{\mathrm{acc}}$) and electric chiller ($Q_{i,t}^{\mathrm{ecc}}$) plus transmitted from other microgrids ($Q_{j,i,t}^{\mathrm{mbtr}}$). The right (demand) side of the cooling demand includes the building's cooling demand ($Q_{i,t}^{\mathrm{bcl}}$) and transmits to other microgrids ($Q_{i,j,t}^{\mathrm{mbtr}}$). L_{pipe} represents the transmission loss of cooling energy within the microgrids.

$$Q_{i,t}^{re} + Q_{i,t}^{bo} + Q_{i,t}^{hp} = Q_{i,t}^{\mathrm{ach}} + Q_{i,t}^{\mathrm{bhl}}, \forall i, t, j, \tag{3}$$

$$Q_{i,t}^{acc} + Q_{i,t}^{ecc} + Q_{j,i,t}^{\mathrm{mbtr}} = Q_{i,t}^{\mathrm{bel}} + Q_{i,j,t}^{\mathrm{mbtr}} \left(1 - L_{\mathrm{pipe}}\right), \forall i, t, j \ne i. \tag{4}$$

Table 1: Indexes, parameters, and variables applied in the proposed model.

Nomenclature	
Abbreviations	
COST	Cost
CDE	Carbon dioxide emission
PEC	Primary energy consumption
CCHP	Combined cooling, heating, and power
SOFC	Solid oxide fuel cell
SRI	Solar radiation index
PV	Photovoltaic
EV	Electric vehicle
CS	Charging station
Subscript	
t	Index of the slotted interval, $t = 1, 2, \cdots, T$
i/j	Number of microgrid, $i/j = 1, 2, \cdots, I$
v	Index for the EVs, $v = 1, 2, ..., V$
Parameters	
P^{NG}	Natural gas price ($/kWh)
P^{maint}	Maintenance price of devices ($/kWh)
P_t^{im}	Electricity price form power grid at time t ($/kWh)
P_t^{ex}	Selling price of electricity to power grid at time t ($/kWh)
α^{NG}	Carbon dioxide emission factor for natural gas (kg/kWh)
α^{grid}	Carbon dioxide emission factor for power grid (kg/kWh)
δ^{NG}	Primary energy conversion parameter for natural gas
δ^{grid}	Primary energy conversion parameter for power grid
δ^{solar}	Primary energy conversion parameter for solar
CAP^{grid}	The limit of power grid (kWh)
CAP_i^{fc}	The capacity of SOFC in microgrid i (kWh)
CAP_i^{bo}	The capacity of boiler in microgrid i (kWh)
CAP_i^{ac}	The capacity of absorption chiller in microgrid i (kWh)
CAP_i^{ec}	The capacity of electric chiller in microgrid i (kWh)
CAP_i^{hp}	The capacity of heat pump in microgrid i (kWh)
CAP_i^{bpv}	The capacity of building's PV in microgrid i (kWh)
CAP_i^{cspv}	The capacity of CS's PV in microgrid i (kWh)
$\text{CAP}_{i,v}^{ev}$	The capacity of CS's EV v in microgrid i (kWh)
SR_t	Solar radiation at time t
$E_{i,t}^{bel}$	Electric load of building in microgrid i at time t
$Q_{i,t}^{\text{bhl}}$	Heating load of building in microgrid i at time t
$Q_{i,t}^{\text{bcl}}$	Cooling load of building in microgrid i at time t
η^{bpv}	Electricity generation efficiency of building's PV
η^{fc}	Electricity generation efficiency of SOFC
η^{re}	Heating generation efficiency of SOFC
η^{ac}	Cooling generation efficiency of absorption chiller
η^{ec}	Cooling generation efficiency of electric chiller
η^{bo}	Heating generation efficiency of boiler
η^{hp}	Heating generation efficiency of heat pump
η^{cspv}	Electricity generation efficiency of CS's PV
$\text{SOC}_{i,v}^{ev\min}$	Minimal electricity store rate of EV v in microgrid i
$\text{SOC}_{i,v}^{ev\max}$	Maximal electricity store rate of EV v in microgrid i
$\text{SOC}_{i,v}^{\text{ini}}$	Initial battery electricity rate of EV v in microgrid i
$\text{SOC}_{i,v}^{\text{des}}$	Demand electricity level at departure time of EV v in microgrid i
Δt	1 h time interval
$\alpha_{i,v}^{c\min}$	Minimal charging limit of EV v in microgrid i
$\alpha_{i,v}^{c\max}$	Maximal charging limit of EV v in microgrid i
$\alpha_{i,v}^{dc\min}$	Minimal discharging limit of EV v in microgrid i
$\alpha_{i,v}^{dc\max}$	Maximal discharging limit of EV v in microgrid i
L_{wire}	Transmission loss of electricity
L_{pipe}	Transmission loss of cooling

Table 1: Continued.

Nomenclature	
Parameters	
M	A big enough number
Continuous decision variables (in time t)	
$\mathrm{NG}_{i,t}^{fc}$	Natural gas consumption of SOFC in microgrid i
$NG_{i,t}^{bo}$	Natural gas consumption of boiler in microgrid i
$E_{i,t}^{fc}$	Electricity generation of SOFC in microgrid i
$E_{i,t}^{\mathrm{bpv}}$	Electricity generation of building's PV in microgrid i
$E_{i,t}^{\mathrm{cspv}}$	Electricity generation of CS's PV in microgrid i
$E_{i,t}^{gb}$	Electricity flow from power grid to building in microgrid i
$E_{i,t}^{\mathrm{gcs}}$	Electricity flow from power grid to CS in microgrid i
$E_{i,t}^{bg}$	Electricity flow from building in microgrid i to power grid
$E_{i,t}^{\mathrm{csg}}$	Electricity flow from CS in microgrid i to power grid
$E_{i,t}^{csb}$	Electricity flow from CS to building in microgrid i
$E_{i,t}^{ec}$	The electricity generated by electric chiller in microgrid i
$E_{i,t}^{hp}$	The electricity consumption by heat pump in microgrid i
$E_{i,j,t}^{\mathrm{mbtr}}$	Electricity exchanged from microgrid i to building in microgrid j
$E_{i,t}^{\mathrm{bcs}}$	Electricity exchanged from building to CS in the microgrid i
$E_{i,t}^{\mathrm{csg}}$	Electricity exchanged from CS to power grid in microgrid i
$E_{i,t}^{\mathrm{csb}}$	Electricity exchanged from CS to building in microgrid i
$E_{i,t}^{cs}$	Electricity needed by CS in microgrid i
$E_{i,j,t}^{\mathrm{mcstr}}$	Electricity exchanged from microgrid i to CS in microgrid j
$E_{i,v,t}^{\mathrm{evc}}$	Electric energy charged to EV v in microgrid i
$E_{i,v,t}^{\mathrm{evdc}}$	Electric energy discharged from EV v in microgrid i
$E_{i,v,t}^{ev}$	Electric energy stored in EV v in microgrid i
$Q_{i,t}^{bo}$	Heat generated from boiler in microgrid i
$Q_{i,t}^{hp}$	Heat generated from heat hump in microgrid i
$Q_{i,t}^{\mathrm{ecc}}$	Cooling generated by electric chiller in microgrid i
$Q_{i,t}^{\mathrm{acc}}$	Cooling generated by absorption chiller in microgrid i
$Q_{i,t}^{re}$	Heating recovered from SOFC in microgrid i
$Q_{i,t}^{ach}$	Heating consumption by absorption chiller in microgrid i
$Q_{i,j,t}^{\mathrm{mbtr}}$	Cooling exchanged from microgrid i to building in microgrid j
Binary decision variables (in time t)	
$x_{i,v,t}^{evc}$	Charging state of EV v in microgrid i
$x_{i,v,t}^{\mathrm{evdc}}$	Discharging state of EV v in microgrid i
$x_{i,t}^{im}$	1 if electricity imported from power grid to microgrid i; 0 otherwise
$x_{i,t}^{ex}$	1 if electricity exported to power grid from microgrid i; 0 otherwise
$x_{i,j,t}^{mb}$	1 if electricity flow from microgrid i to building in microgrid j; 0 otherwise
$x_{i,j,t}^{\mathrm{mcs}}$	1 if electricity flow from microgrid i to CS in microgrid j; 0 otherwise
$x_{i,j,t}^{\mathrm{mbc}}$	1 if cooling flow from microgrid i to building in microgrid j; 0 otherwise

(c) *Constraints for PV*. Electricity generated by PV panel ($E_{i,t}^{\mathrm{bpv}}$) can be calculated by its size ($\mathrm{CAP}_i^{\mathrm{bpv}}$) multiplying by electricity generation efficiency (η^{bpv}) and solar radiation (SR_t) in microgrid i as follows:

$$E_{i,t}^{\mathrm{bpv}} \leq \mathrm{CAP}_i^{\mathrm{bpv}} \times \eta^{\mathrm{bpv}} \times SR_t, \forall i, t, i. \quad (5)$$

(d) *Constraints for CCHP*. The electric/thermal output of SOFC ($E_{i,t}^{fc}$), boiler ($Q_{i,t}^{bo}$), absorption chiller ($Q_{i,t}^{\mathrm{acc}}$), electric chiller ($Q_{i,t}^{\mathrm{ecc}}$), and heat pump ($Q_{i,t}^{hp}$) must be not more than the corresponding installed capacities (CAP) in microgrid i as given in equations (6)–(10). The energy conversion efficiencies are given in

equations (11)–(16), where η shows the energy efficiency of various devices in the CCHP system.

$$E_{i,t}^{fc} \le \mathrm{CAP}_i^{fc} \forall i,t, \tag{6}$$

$$Q_{i,t}^{bo} \le \mathrm{CAP}_i^{bo} \forall i,t, \tag{7}$$

$$Q_{i,t}^{\mathrm{acc}} \le \mathrm{CAP}_i^{ac} \forall i,t, \tag{8}$$

$$Q_{i,t}^{\mathrm{ecc}} \le \mathrm{CAP}_i^{ec} \forall i,t, \tag{9}$$

$$Q_{i,t}^{hp} \le \mathrm{CAP}_i^{hp} \forall i,t, \tag{10}$$

$$E_{i,t}^{fc} = \eta^{fc} \times NG_{i,t}^{fc} \forall i,t, \tag{11}$$

$$Q_{i,t}^{re} = \eta^{re} \times E_{i,t}^{fc} \forall i,t, \tag{12}$$

$$Q_{i,t}^{\mathrm{acc}} = \eta^{ac} \times Q_{i,t}^{\mathrm{ach}} \forall i,t, \tag{13}$$

$$Q_{i,t}^{\mathrm{ecc}} = \eta^{ec} \times E_{i,t}^{ec} \forall i,t, \tag{14}$$

$$Q_{i,t}^{bo} = \eta^{bo} \times NG_{i,t}^{bo} \forall i,t, \tag{15}$$

$$Q_{i,t}^{hp} = \eta^{hp} \times E_{i,t}^{hp} \forall i,t. \tag{16}$$

3.1.3. Electric Vehicle Charging Station Operation Decision Model

(a) *Electric Load Balance Constraints.* Constraint in equation (17) represents that the supply and demand of electricity should be equal at time t for CS in microgrid i. For microgrid i, the energy suppliers include purchased from utility grid ($E_{i,t}^{\mathrm{gcs}}$), transmitted from building ($E_{i,t}^{\mathrm{bcs}}$), generated by CS's PV ($E_{i,t}^{\mathrm{cspv}}$), and transmitted from other microgrids j ($E_{j,i,t}^{\mathrm{mcstr}}$). The energy demand includes electricity sold back to the utility grid ($E_{i,t}^{\mathrm{csg}}$), transmitted to other buildings ($E_{i,t}^{\mathrm{csb}}$), requested energy to charge EVs ($E_{i,t}^{cs}$), and transmitted to other microgrid j ($E_{i,j,t}^{\mathrm{mcstr}}$). Constraint (18) means that electricity requested energy to charge EVs equals to the EVs' charging minus discharging energy.

$$\begin{aligned} E_{i,t}^{\mathrm{gcs}} + E_{i,t}^{\mathrm{bcs}} + E_{i,t}^{\mathrm{cspv}} + \sum_j E_{j,i,t}^{\mathrm{mcstr}} \times (1 - L_{wire}) \\ = E_{i,t}^{\mathrm{csg}} + E_{i,t}^{\mathrm{csb}} + E_{i,t}^{cs} + \sum_j E_{i,j,t}^{\mathrm{mcstr}} \quad \forall i,t, \end{aligned} \tag{17}$$

$$E_{i,t}^{\mathrm{csev}} = \sum_v \left(E_{i,v,t}^{\mathrm{evc}} - E_{i,v,t}^{\mathrm{evdc}} \right) \forall i,t. \tag{18}$$

(b) *Constraints for PV.* Similarly, electricity generated by CS's PV panel ($E_{i,t}^{\mathrm{cspv}}$) is restrained by its capacity ($\mathrm{CAP}_i^{\mathrm{cspv}}$) times electricity generating efficiency (η^{cspv}) and solar radiation (SR_t) in microgrid i.

$$E_{i,t}^{\mathrm{cspv}} \le CAP_i^{\mathrm{cspv}} \times \eta^{\mathrm{cspv}} \times SR_t \forall i,t. \tag{19}$$

(c) *Constraints for Electric Vehicles.* For the EVs, $T_{i,v}^{a}$ and $T_{i,v}^{ua}$ represent the EV v arriving and leaving the CS in microgrid i, which are assumed as available and unavailable time, respectively. During the EV parking time (available time), the thermal energy stored in EVs ($E_{i,v,t+1}^{ev}$) is bounded as shown in equation (20) and can be calculated by charging energy minus discharging energy as displayed in equations (21) and (22). Constraint (23) guarantees the electricity level of EV ($E_{i,v,t-1}^{ev}$) which can meet the owner's desired electricity level when the EV leaves the CS. Equation (24) designates that EVs cannot be in charging ($x_{i,v,t}^{\mathrm{evc}}$) and discharging ($x_{i,v,t}^{\mathrm{evdc}}$) states at the same time. Constraints (25) and (26) are used to guarantee that the EV battery charging and discharging electricity are limited by their maximum and minimum charging and discharging rate, respectively.

$$\mathrm{CAP}_{i,v}^{ev} \times SOC_{i,v}^{\mathrm{evmin}} \le E_{i,v,t}^{ev} \le CAP_{i,v}^{ev} \times SOC_{i,v}^{\mathrm{evmax}} \forall i,v,T_{i,v}^{a} \le t \le T_{i,v}^{ua}, \tag{20}$$

$$E_{i,v,t+1}^{ev} = \mathrm{CAP}_{i,v}^{ev} \times \mathrm{SOC}_{i,v}^{\mathrm{ini}} + \left(E_{i,v,t+1}^{\mathrm{evc}} - E_{i,v,t+1}^{\mathrm{evdc}} \right) \times \Delta t \forall i,v,t = T_{i,v}^{a}, \tag{21}$$

$$E_{i,v,t+1}^{ev} - E_{i,v,t}^{ev} = \left(E_{i,v,t+1}^{\mathrm{evc}} - E_{i,v,t+1}^{\mathrm{evdc}} \right) \times \Delta t \forall i,v,T_{i,v}^{a} < t < T_{i,v}^{ua}, \tag{22}$$

$$E_{i,v,t-1}^{ev} \ge \mathrm{CAP}_{i,v}^{ev} \times \mathrm{SOC}_{i,v}^{\mathrm{des}} \forall i,v,t = T_{i,v}^{ua}, \tag{23}$$

$$x_{i,v,t}^{\mathrm{evc}} + x_{i,v,t}^{\mathrm{evdc}} \le 1 \forall i,v,T_{i,v}^{a} < t < T_{i,v}^{ua}, \tag{24}$$

$$\mathrm{CAP}_{i,v}^{ev} \times \alpha_{i,v}^{\mathrm{cmin}} \times x_{i,v,t}^{evc} \le E_{i,v,t}^{\mathrm{evc}} \le \mathrm{CAP}_{i,v}^{ev} \times \alpha_{i,v}^{\mathrm{cmax}} \times x_{i,v,t}^{\mathrm{evc}} \forall i,v,T_{i,v}^{a} < t < T_{i,v}^{ua}, \tag{25}$$

$$\mathrm{CAP}_{i,v}^{ev} \times \alpha_{i,v}^{\mathrm{dcmin}} \times x_{i,v,t}^{\mathrm{evdc}} \le E_{i,v,t}^{evdc} \le \mathrm{CAP}_{i,v}^{ev} \times \alpha_{i,v}^{\mathrm{dcmax}} \times x_{i,v,t}^{\mathrm{evdc}} \forall i,v,T_{i,v}^{a} < t < T_{i,v}^{ua}. \tag{26}$$

3.1.4. Constraints for Grid Exchange. Constraint (27) indicates that electricity cannot be imported from and exported to power grid at the same time for the microgrid. Equation (28) ensures that electricity from utility grid and CS are restricted by maximum capacity. Similarly, equation (29) states that electricity feed-in utility grid and CS are restricted by maximum capacity.

$$x_{i,t}^{im} + x_{i,t}^{ex} \le 1 \forall i, t, \tag{27}$$

$$E_{i,t}^{bg} + E_{i,t}^{\text{csg}} \le x_{i,t}^{ex} \times \text{CAP}^{\text{grid}} \forall i, t, \tag{28}$$

$$E_{i,t}^{gb} + E_{i,t}^{\text{gcs}} \le x_{i,t}^{im} \times \text{CAP}^{\text{grid}} \forall i, t. \tag{29}$$

3.1.5. Constraints for Networking. The constraint expressed in equations (30), (33), and (36) indicates that electricity/cooling feed-in and import cannot happen simultaneously. Note that $x_{i,j,t}^{mb}$ and $x_{i,j,t}^{\text{mcs}}$ are binary variables to represent the electricity from buildings and CS in microgrids i to j exchange status, respectively. The transmission of electricity energy ($E_{i,j,t}^{\text{mbtr}}$, $E_{j,i,t}^{\text{mbtr}}$) restricted by exchange status is defined in equations (31), (32), (34), and (35). $x_{i,j,t}^{mbc}$ is binary variable to control the cooling in building from microgrids i to j exchange status. Constraints (37) and (38) ensure that the transmission of cooling energy ($Q_{i,j,t}^{\text{mbtr}}$, $Q_{j,i,t}^{\text{mbtr}}$) is limited by exchange status. M is a big number, normally adopted in mixed integer programming.

$$x_{j,i,t}^{mb} + x_{i,j,t}^{mb} \le 1 \forall i, t, j \ne i, \tag{30}$$

$$E_{j,i,t}^{\text{mbtr}} \le M \times x_{j,i,t}^{mb} \forall i, t, j \ne i, \tag{31}$$

$$E_{i,j,t}^{\text{mbtr}} \le M \times x_{i,j,t}^{mb} \forall i, t, j \ne i, \tag{32}$$

$$x_{j,i,t}^{\text{mcs}} + x_{i,j,t}^{\text{mcs}} \le 1 \forall i, t, j \ne i \tag{33}$$

$$E_{j,i,t}^{\text{mcstr}} \le M \times x_{j,i,t}^{\text{mcs}} \forall i, t, j \ne i, \tag{34}$$

$$E_{i,j,t}^{\text{mcstr}} \le M \times x_{i,j,t}^{\text{mcs}} \forall i, t, j \ne i, \tag{35}$$

$$x_{j,i,t}^{\text{mbc}} + x_{i,j,t}^{\text{mbc}} \le 1 \forall i, t, j \ne i, \tag{36}$$

$$Q_{j,i,t}^{\text{mbtr}} \le M \times x_{j,i,t}^{\text{mbc}} \forall i, t, j \ne i, \tag{37}$$

$$Q_{i,j,t}^{\text{mbtr}} \le M \times x_{i,j,t}^{\text{mbc}} \forall i, t, j \ne i. \tag{38}$$

3.2. Objectives. In this study, three objectives are evaluated from the economic, environmental, and energy saving perspective, respectively.

3.2.1. Operational Cost (COST). The collective interest of the microgrids can be formulated as equation (39a), which is to minimize the sum of each microgrid's energy cost as equation (39b). As shown in equation (39b), the energy cost of each microgrid can be subdivided into cost associated with natural gas (the first term), maintenance cost of equipment (the second term), costs associated with power grids (the third term), and revenue associated with utility grids (the last term).

$$\min f^{\text{COST}} = \sum_i \text{COST}_i, \tag{39a}$$

$$\begin{aligned} \text{COST}_i \quad &= P^{NG} \times \sum_t \left(NG_{i,t}^{fc} + NG_{i,t}^{bo} \right) + P^{\text{maint}} \times \sum_t \left(E_{i,t}^{fc} + E_{i,t}^{\text{bpv}} + E_{i,t}^{\text{cspv}} + Q_{i,t}^{bo} + Q_{i,t}^{hp} + Q_{i,t}^{\text{ecc}} + Q_{i,t}^{\text{acc}} \right) \\ &\quad + P_t^{im} \times \sum_t \left(E_{i,t}^{gb} + E_{i,t}^{\text{gcs}} \right) - P_t^{ex} \times \sum_t \left(E_{i,t}^{bg} + E_{i,t}^{\text{csg}} \right) \forall i. \end{aligned} \tag{39b}$$

3.2.2. Carbon Dioxide Emission (CDE). Greenhouse gases from the power generation combusting fuel deteriorate the environment, in which global warming is one of the crucial issues. The CDE is selected as the environmental index, and the collective environmental benefit of the microgrids can be built as equation (40a), with the aim of minimizing the sum of each microgrid's CDE as equation (40b). As displayed in equation (40b), the CDE of each microgrid can be estimated by the emissions from natural gas consumption (the first term) and purchased electricity from the utility grid (the second term).

$$\min f^{\text{CDE}} = \sum_i \text{CDE}_i, \tag{40a}$$

$$\text{CDE}_i = \alpha^{NG} \times \sum_t \left(NG_{i,t}^{fc} + NG_{i,t}^{bo} \right) + \alpha^{\text{grid}} \times \sum_t \left(E_{i,t}^{gb} + E_{i,t}^{\text{gcs}} \right). \tag{40b}$$

3.2.3. Primary Energy Consumption (PEC). The collective energy benefit of the microgrids can be formulated as equation (41a), which is to minimize the sum of each microgrid's PEC as equation (41b). The PEC of each microgrid includes primary energy consumption of natural gas (the first term), utility grid (the second term), and PV panel (the last term), as shown in equation (41b).

$$\min f^{\mathrm{PEC}} = \sum_i \mathrm{PEC}_i, \tag{41a}$$

$$\mathrm{PEC}_i = \delta^{NG} \times \sum_t \left(NG_{i,t}^{fc} + NG_{i,t}^{bo}\right) + \delta^{\mathrm{grid}} \times \sum_t \left(E_{i,t}^{gb} + E_{i,t}^{\mathrm{gcs}}\right) + \delta^{\mathrm{solar}} \times \sum_t \left(E_{i,t}^{\mathrm{bpv}} + E_{i,t}^{\mathrm{cspv}}\right). \tag{41b}$$

3.3. Multiobjective Optimization. The multiobjective optimization (MOO) algorithm is substantially different from single-objective optimization since there are various but conflicting evaluation indicators in MOO. The weighting method uses weights to represent the goals preferred by decision makers [30], which is adopted to solve the proposed model after normalization in this paper.

3.3.1. Normalization of Indicators. In equation (42), three indicators have different units and characteristics, in which f represents an objective and f^{non} shows the normalized objective calculated by

$$f^{\mathrm{non}} = \begin{cases} 1, & f \le f^-, \\ \dfrac{f - f^-}{f^+ - f^-}, & f^- \le f \le f^+, \\ 0, & f \ge f^+, \end{cases} \tag{42}$$

where $f^- = \min\{f\}$ and $f^+ = \max\{f\}$.

3.3.2. Weighting Method. After normalization of these indicators and using the weighting method, the multiobjective model can be transformed into the following single-objective model:

$$\min f = \omega_1 f^{\mathrm{COST,non}} + \omega_2 f^{\mathrm{CDE,non}} + \omega_3 f^{\mathrm{PEC,non}}, \tag{43}$$

where ω represents the weight of objective, which will determine the solution of the fitness function and show the performance priority. Different weighting scenarios represent the preferences of decision makers in different contexts.

4. Operation Decision Models for Transactive Energy Management

To carry out this analysis, the proposed model (i.e., model III) balancing global and local benefits is compared with two reference models (i.e., models I and II). Reference model I is presented to search for the total benefit for all the microgrids that are disconnected and operated separately, which is used to compare the performance of the microgrids with single microgrid operation. The global microgrids are obtained in the reference model II integrating V2G and V2B, when each microgrid can freely connect with other microgrids to share information and exchange energy in the transactive energy work.

4.1. Reference Model I. The mathematic model is formulated as reference model and f^I is the total performance for the microgrids. Constraint (45) ensures that there is no energy exchange among microgrids, buildings, and charging stations.

Reference model I:

$$\min f^I = \omega_1 \times f^{I,\mathrm{COST,non}} + \omega_2 \times f^{I,\mathrm{CDE,non}} + \omega_3 \times f^{I,\mathrm{PEC,non}}, \tag{44}$$

$$\mathrm{s.t}\, x_{j,i,t}^{mb} = 0 x_{i,j,t}^{mb} = 0; x_{j,i,t}^{\mathrm{mcs}} = 0; x_{i,j,t}^{\mathrm{mcs}} = 0; x_{j,i,t}^{mb} = 0; x_{i,j,t}^{mb} = 0, \forall i, t, j \ne i. \tag{45}$$

Equations (45) and (1)–(38) compose the constraints for reference model I jointly.

4.2. Reference Model II. In this operation model, reference model II is built to study the operation decisions for the microgrids with the aim to obtain global microgrids benefit, when energy can freely exchange among microgrids. In this model, maximizing the global collective benefit of the microgrids is the focus and a MILP model is formulated to obtain the operation decisions for the microgrids.

Reference model II:

$$\min f^{II} = \omega_1 \times f^{II,\mathrm{COST,non}} + \omega_2 \times f^{II,\mathrm{CDE,non}} + \omega_3 \times f^{II,\mathrm{PEC,non}}. \tag{46}$$

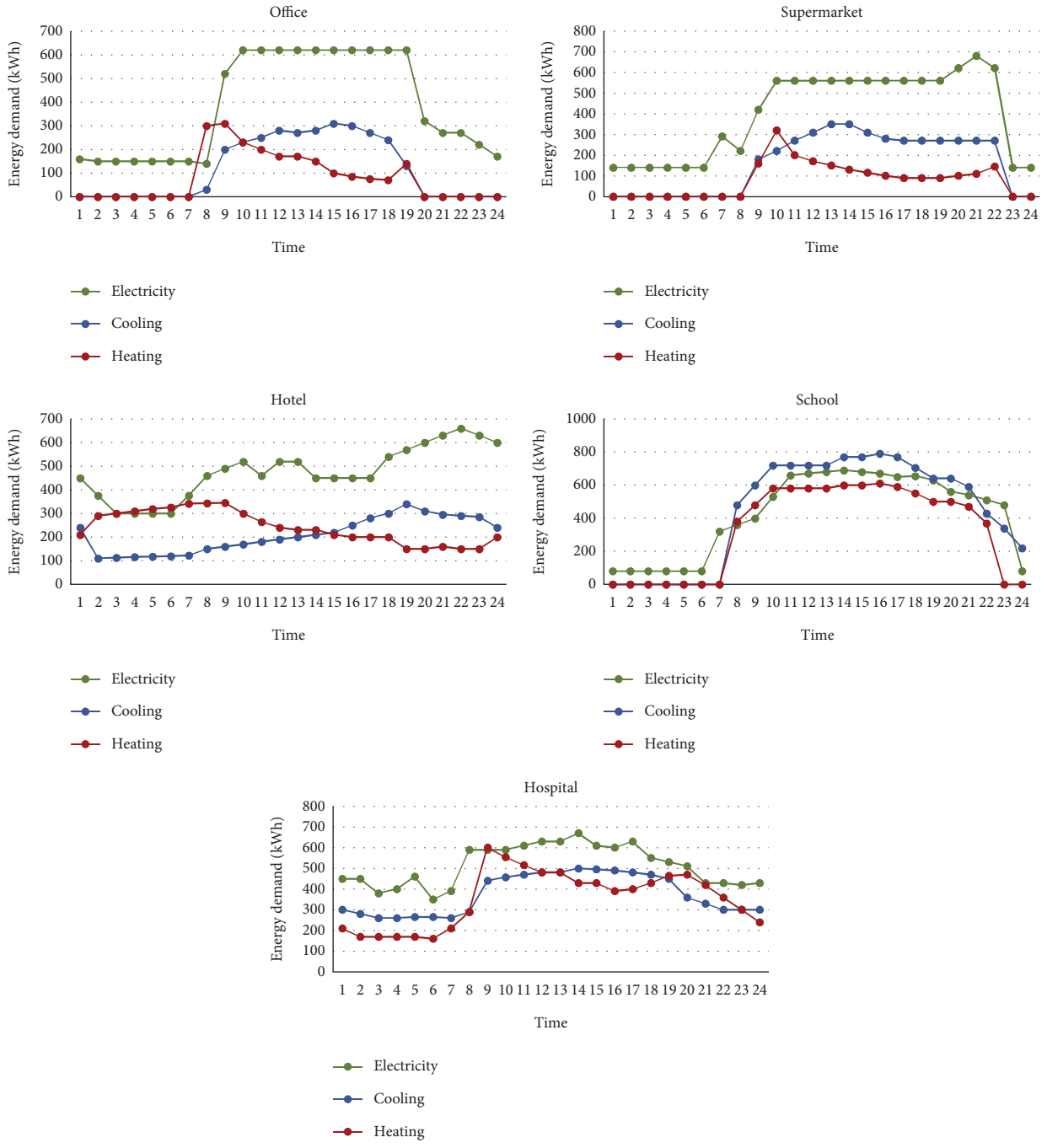

Figure 3: Typical weekday electricity heating and cooling demand profiles of five buildings in the microgrids located in Shanghai.

Equations (1)–(38) compose the constraints for reference model II.

4.3. Model III. Although the reference model II can minimize the collective interests, the individual interests of each microgrid may not be ensured. That is to say, some microgrids may have to spend more if they join the clusters. For a profit-driven entity (i.e., the microgrid's owner), to guarantee each microgrid achieves cost savings in the clusters, reference model II is extended to model III by introducing a constraint in equation (48). α, β, and δ are parameters to indicate the percentage of interest saving regarded as the same level. Furthermore, equations (48)–(50) can be modified to be constraints to guarantee the microgrid's economic, environmental, and energy benefits when microgrid i decision markers pay attention to achieving individual interests.

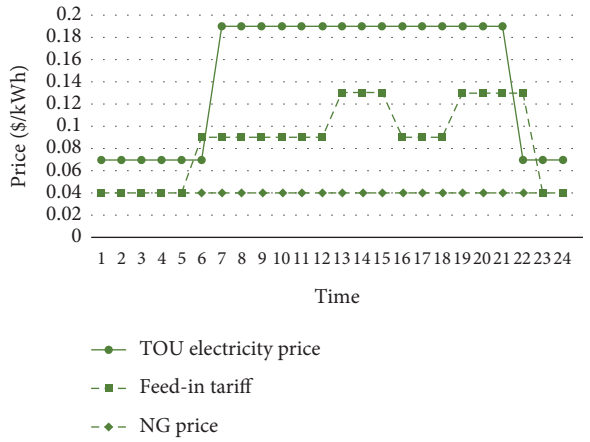

Figure 4: The energy price.

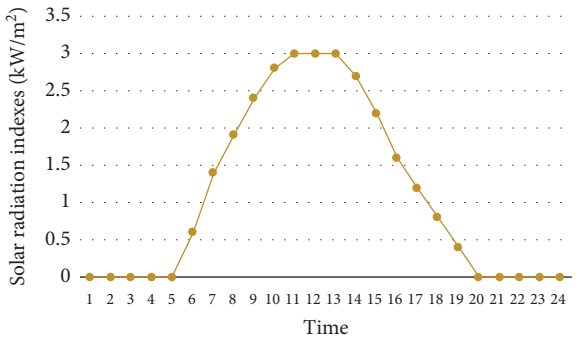

Figure 5: The solar radiation indexes.

Table 2: The EVs arriving and leaving time of five buildings in the microgrids.

	Office	Supermarket	Hotel	School	Hospital
Arriving time	8 : 00	18 : 00	1 : 00	7 : 00	1 : 00
Leaving time	17 : 00	23 : 00	8 : 00	19 : 00	24 : 00

Table 3: Description of parameter settings [29, 30, 32–35].

Category	Notation	Value
Technical input	η^{fc}	0.45
	η^{re}	0.37
	η^{ac}	1
	η^{ec}	4
	η^{bo}	0.85
	η^{hp}	3.5
	η^{bpv}	0.18
	η^{cspv}	0.18
	L_{wire}	0.05
	L_{pipe}	0.06
	$\text{SOC}_{i,v}^{\text{evmin}}$	0.10
	$\text{SOC}_{i,v}^{\text{evmax}}$	1
	$\alpha_{i,v}^{c\,\min}$	0.05
	$\alpha_{i,v}^{c\max}$	0.25
	$\alpha_{i,v}^{dc\min}$	0.05
	$\alpha_{i,v}^{dc\max}$	0.25
	$\text{SOC}_{i,v}^{\text{ini}}$	0.2
	$\text{SOC}_{i,v}^{\text{evd}}$	1
Capacity input	$\text{CAP}_{i,v}^{ev}$	30 kWh
	CAP^{grid}	700 kW
	$\text{CAP}_i^{\text{bpv}}$	1000 m^2
	CAP_i^{fc}	580 kW
	CAP_i^{bo}	1500 kW
	CAP_i^{ac}	1200 kW
	CAP_i^{ec}	1200 kW
	CAP_i^{hp}	1200 kW
	$\text{CAP}_i^{\text{cspv}}$	200 m^2
Economic input	P^{maint}	0.0015 $/kWh
Environment input	α^{NG}	0.18 kg/kWh
	α^{grid}	0.95 kg/kWh
Energy input	δ^{NG}	1.047
	δ^{solar}	0.9
	δ^{grid}	3.336

Model III:

$$\min f^{III} = \omega_1 \times f^{III,\text{COST,non}} + \omega_2 \times f^{III,\text{CDE,non}} + \omega_3 \times f^{III,\text{PEC,non}}, \tag{47}$$

$$\text{s.t. } f_i^{III,\text{COST,non}} \le f_i^{I,\text{COST,non}} \times (1-\alpha)\forall i, \tag{48}$$

$$f_i^{III,\text{CDE,non}} \le f_i^{I,\text{CDE,non}} \times (1-\beta)\forall i, \tag{49}$$

$$f_i^{III,\text{PEC,non}} \le f_i^{I,PEC,non} \times (1-\delta)\forall i, \tag{50}$$

Constraints in equations (1)–(38)

5. Case Study

To validate the economic, environmental, and energy criteria of the proposed system using the multiobjective models built, the microgrids in Shanghai, China, are investigated as a case study. In this research, the decision time interval is set at 1 h. The microgrids consisting of five public building categories (i.e., hotel, office, hospital, school, and supermarket) are selected for analysis in the case. The typical weekday hourly energy demand profiles including electric,

Table 4: Performances of each microgrid in the microgrids for reference models I-II and model III in the neutral scenario.

Microgrid index	COST ($)			CDE (tons)			PEC ($*10^4$)		
	Reference model I	Reference model II	Model III	Reference model I	Reference model II	Model III	Reference model I	Reference model II	Model III
1	429.88	452.39	429.88	3.31	1.93	1.83	2.00	1.65	1.59
2	447.36	478.84	447.36	3.05	2.05	1.92	2.03	1.71	1.64
3	705.30	716.52	705.30	3.50	3.08	3.04	2.54	2.32	2.29
4	834.35	763.31	834.35	4.20	3.23	3.55	2.84	2.41	2.59
5	933.55	946.04	933.55	4.40	4.06	4.08	3.08	2.89	2.90
Overall	3350.44	3357.10	3350.44	18.46	14.35	14.42	12.49	10.98	11.01

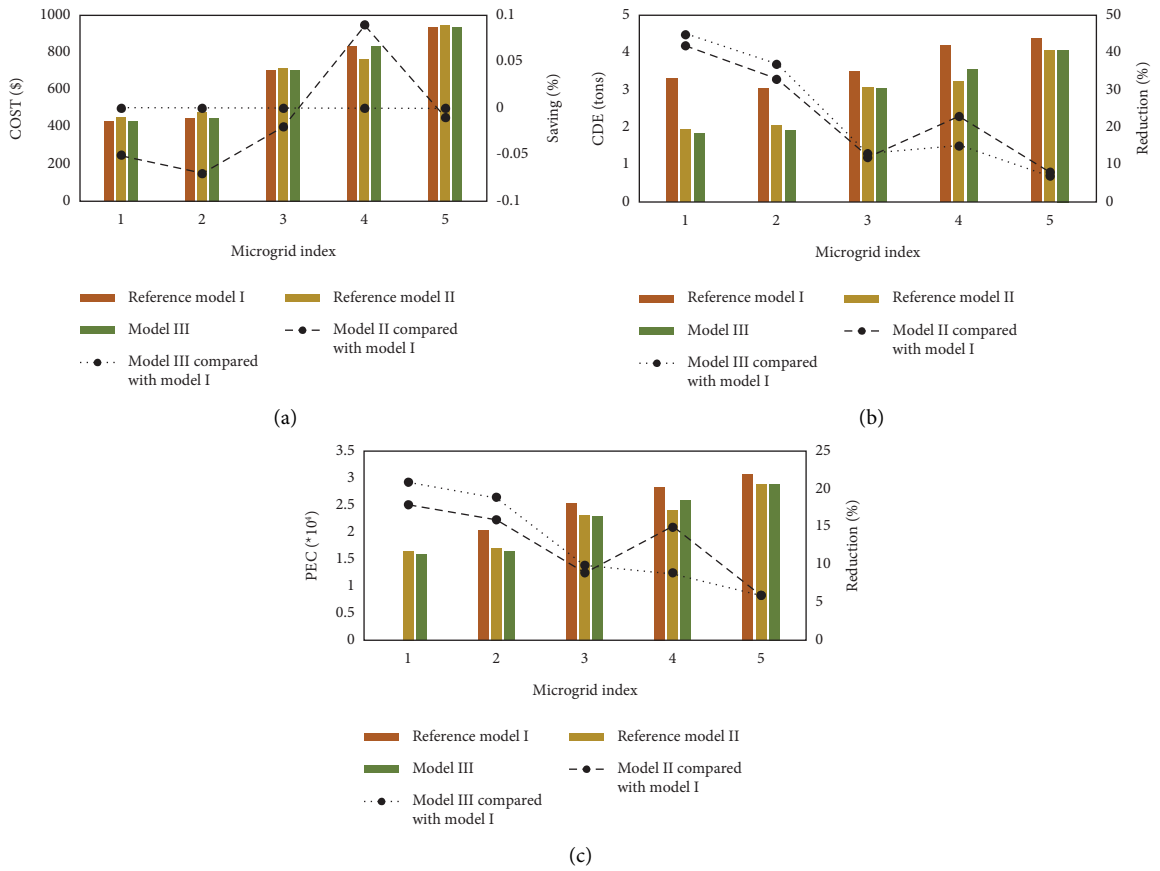

Figure 6: Saving performances of each microgrid in the microgrids for reference models I-II and model III in the neutral scenario: (a) COST. (b) CDE. (c) PEC.

heating, and cooling of each building in the transition season are plotted in Figure 3 [31]. The TOU energy prices are displayed in Figure 4 [26], and the solar radiation indexes are presented in Figure 5 [32].

For the charging stations, each parking area is set with a maximum capacity of five EVs. Moreover, it is assumed each CS is in full-state during corresponding time interval set to be in Table 2. The EVs arrive at the CS with 20% battery charged and leave with 100% charged battery. Furthermore, other parameters related to the models are given in Table 3.

A computer with an Intel (R) Core (™) i5-8265U CPU @1.60 GHz processor and 8 GB memory running Windows 10 on a 64 bit operating system is used for all experiments. The proposed multiobjective optimization method of transactive energy management is implemented in Python 3. The optimization programming language is adopted to code the mathematical models in IBM ILOG CPLEX v12.8 optimizer. Through the Python API, the optimization models are solved by IBM Decision Optimization CPLEX (DOcplex) Modelling for Python. To verify the models' scalability and feasibility, three operation decision models under four weighting scenarios are examined for economic, environmental, and energy performance in the objective function.

5.1. Neutral Scenario. In the neutral scenario, equal weights (i.e., $\omega_1 = \omega_2 = \omega_3 = 1/3$) are adopted in the operation decision models and represent equal importance for the three objectives. After running the reference models I-II and model III, the economic and environmental as well as energy

Table 5: Performances of each microgrid in the microgrids for reference models I-II and model III in the proeconomic scenario.

Microgrid index	COST ($)			CDE (tons)			PEC (*10^4)		
	Reference model I	Reference model II	Model III	Reference model I	Reference model II	Model III	Reference model I	Reference model II	Model III
1	353.585	286.347	326.44	3.89	3.07	3.07	2.34	2.31	2.31
2	362.474	426.674	340.73	3.70	3.44	3.11	2.41	2.37	2.18
3	611.778	674.822	575.07	4.20	4.57	4.14	2.95	3.03	2.93
4	804.252	650.213	756.00	4.41	3.64	4.18	2.97	2.64	2.80
5	867.95	773.5	815.87	4.88	4.52	4.75	3.36	3.15	3.29
Overall	3000.039	2811.556	2814.11	21.08	19.24	19.25	14.03	13.50	13.51

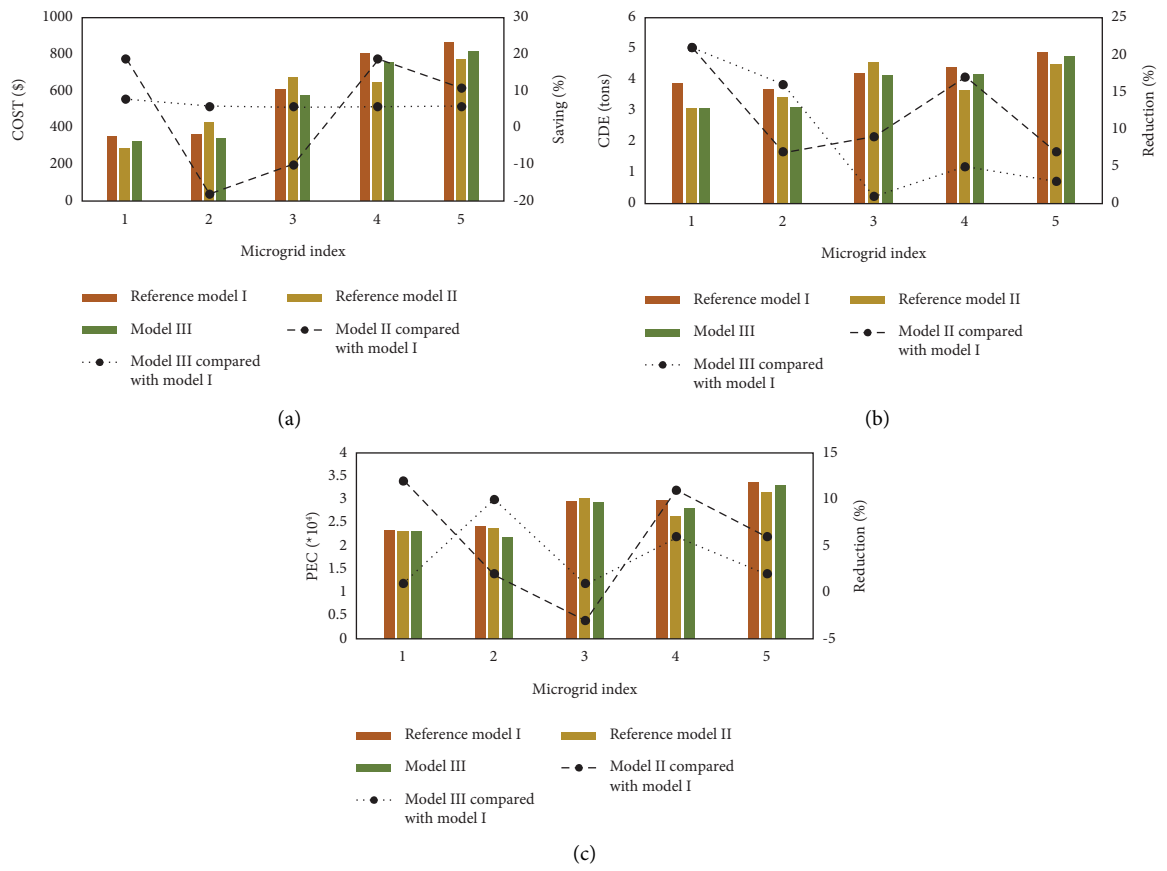

Figure 7: Saving performances of each microgrid in the microgrids for reference models I-II and model III in the proeconomic scenario. (a) COST. (b) CDE. (c) PEC.

performances of each microgrid are recorded in Table 4, and the three models run for 316 seconds. The total COST, CDE, and PEC for the microgrids under reference model I are \$3,350.44, 18.46 tons, and $12.49 * 10^4$, respectively. It is demonstrated that reference model II can achieve about 22% CDE reduction and 12% PEC saving compared with reference model I. Despite the COST of reference models I and II is about the same, each microgrid cost saving level is different. Model III is adopted to obtain an optimal energy strategy while balancing global and single-cost interests with $\alpha = 0$, when the microgrid's entity focuses on economic performance. In addition, β and δ are set to be 0. The results of reference models and model III are shown in Table 4, and the saving/reduction in economic, environmental, and energy performance of each microgrid under different operation models is displayed in Figure 6.

As shown in Table 4, the objective function of three models (i.e., f^I, f^{II}, and f^{III}) under neutral scenario can be known with 0.67, 0.67, and 0.014. Therefore, the proposed method can achieve economic, environmental, and energy benefits simultaneously. In Figure 6, the economic interest of each microgrid can be ensured in the presented model III when the cost of 1-th, 2-th, 3-th, and 5-th microgrid is larger than reference models I. Compared with reference I, the PEC

Table 6: Performances of each microgrid in the microgrids for reference models I-II and model III in the proenvironmental scenario.

Microgrid index	COST ($)			CDE (tons)			PEC ($*10^4$)		
	Reference model I	Reference model II	Model III	Reference model I	Reference model II	Model III	Reference model I	Reference model II	Model III
1	429.88	449.36	605.62	3.31	1.92	2.61	2.00	1.64	2.04
2	447.50	475.87	519.18	3.05	2.03	2.22	2.04	1.71	1.82
3	705.30	715.60	645.63	3.50	3.07	2.77	2.54	2.31	2.13
4	832.90	765.81	781.13	4.19	3.25	3.31	2.86	2.41	2.45
5	933.55	950.47	814.32	4.40	4.08	3.47	3.08	2.90	2.54
Overall	3349.13	3357.1	3365.88	18.45	14.35	14.38	12.52	10.97	10.98

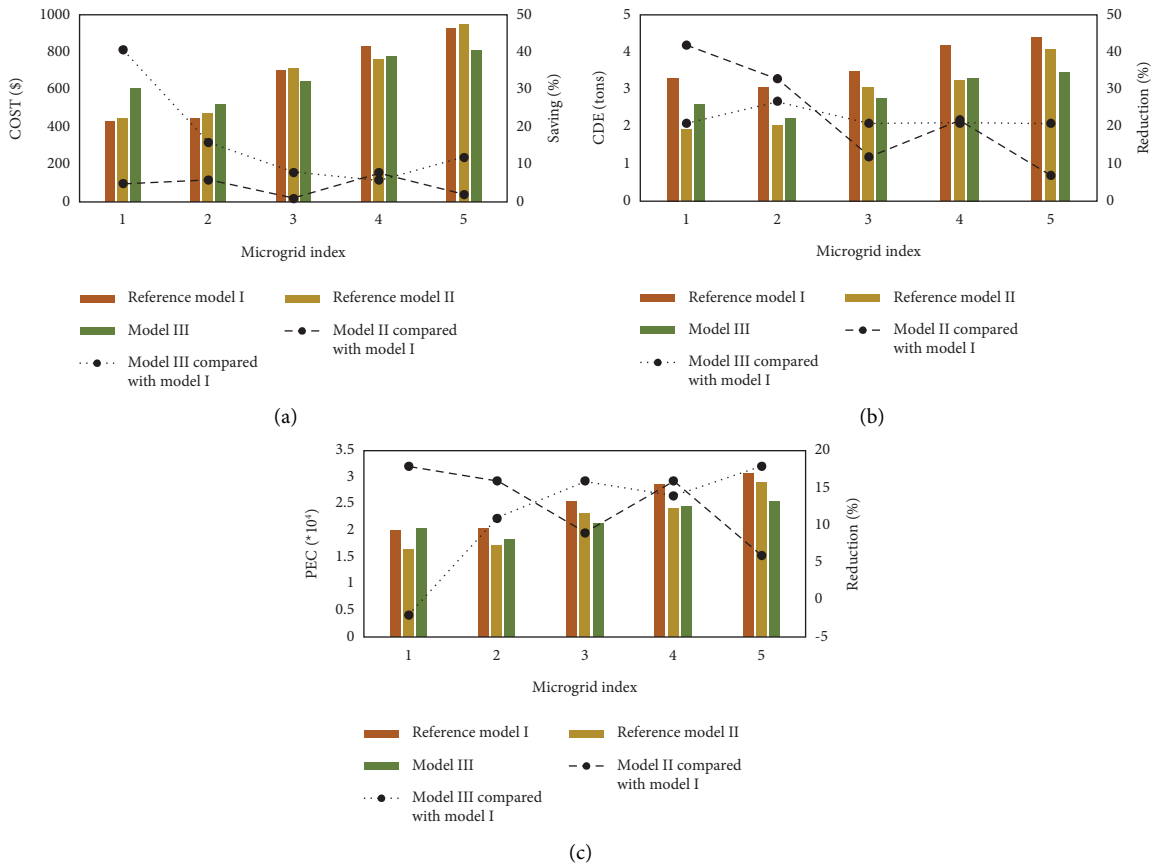

Figure 8: Saving performances of each microgrid in the microgrids for reference models I-II and model III in the proenvironmental scenario. (a) COST. (b) CDE. (c) PEC.

and CDE reduction levels of each microgridare similar in model III and reference model II. Subgraphs (a), (b), and (c) in Figure 6 also show that the economic interests have been equilibrated best. Therefore, as shown in Table 4 and Figure 6, the proposed microgrids integrating V2G and V2B formulated multiobjective model can obtain multibenefits and achieve a balance between global and individual benefits under a neutral scenario.

5.2. Proeconomic Scenario. In the proeconomic scenario, $\omega_1 = 0.8$ and $\omega_2 = \omega_3 = 0.1$ are set to represent the proenvironmental attitude and are used in operation decision models. Table 5 displays the performance of each microgrid under three operation models, and the three models run for 309 seconds. In the reference model II under proeconomic scenario, the centralize collective operation can achieve about 6% COST saving, 9% CDE reduction, and 4% PEC reduction compared with the reference model I. However, the economic benefits of each microgrid may be not ensured, for example, the COST and CDE as well as PEC of 2-th microgrid increased. For proeconomic microgrid entity, constraint ensuring economic benefit are added to the proposed model III. Model III is adopted to guarantee each microgrid can have cost saving with minimum level. α is set up to be an average percentage (i.e., 6%) based on the overall COST saving, and β as well as δ are set be 0.

Table 7: Performances of each microgrid in the microgrids for reference models I-II and model III in the proenergy scenario.

Micro-grid index	COST ($)			CDE (tons)			PEC (*10^4)		
	Reference model I	Reference model II	Model III	Reference model I	Reference model II	Model III	Reference model I	Reference model II	Model III
1	533.98	452.39	480.53	3.31	1.93	2.06	1.90	1.65	1.72
2	547.91	478.84	487.94	3.50	2.05	2.09	1.94	1.71	1.74
3	798.04	721.68	696.07	3.50	3.10	2.99	2.46	2.33	2.26
4	926.34	760.90	795.04	4.27	3.22	3.37	2.73	2.40	2.49
5	1020.91	943.29	898.90	4.40	4.05	3.85	3.00	2.88	2.76
Overall	3827.18	3357.10	3358.48	18.98	14.35	14.36	12.04	10.97	10.97

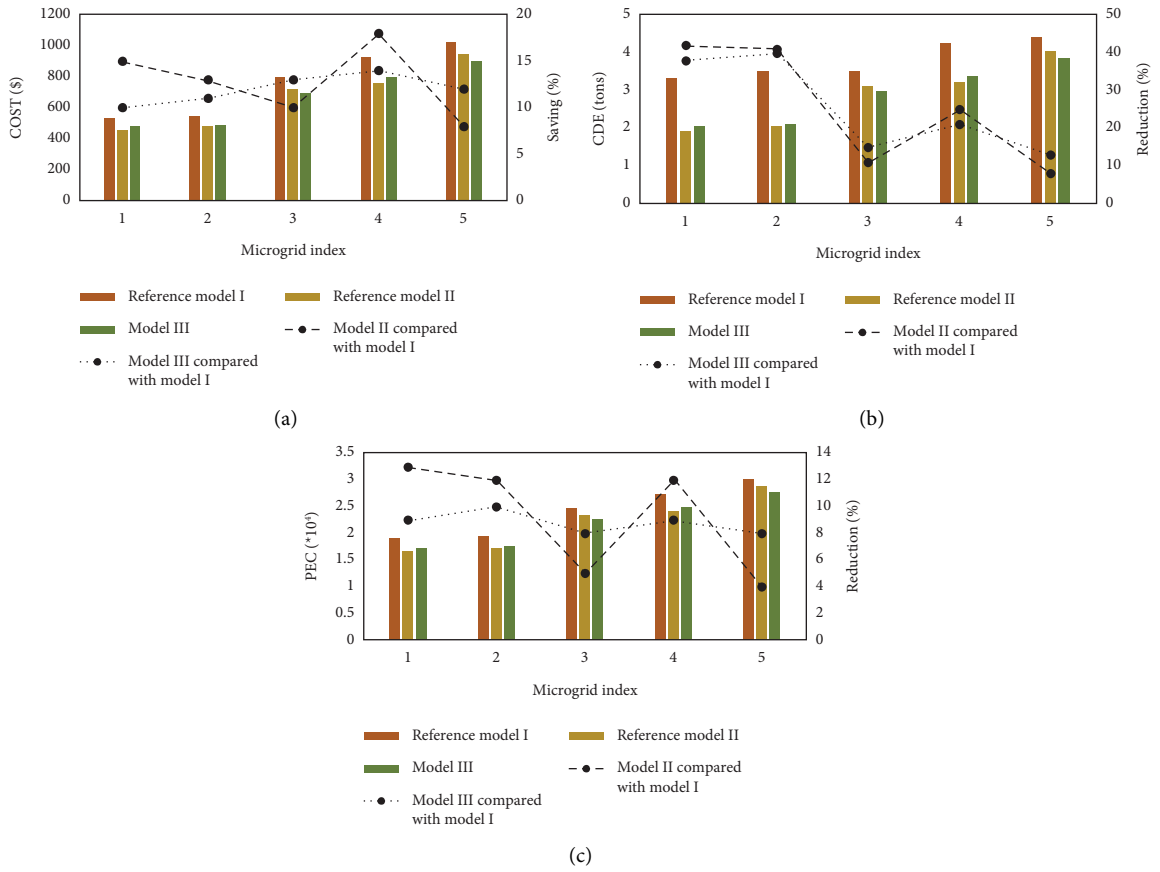

Figure 9: Saving performances of each microgrid in the microgrids for reference models I-II and model III in the proenergy scenario. (a) COST. (b) CDE. (c) PEC.

As shown in Table 5, the value of f^I, f^{II}, and f^{III} under proeconomic weighting scenario can be known with 1, 0, and 0.038. Therefore, the proposed method can get multibenefits similar to reference model II and superior to reference model I under microgrids running alone. In Figure 7, the COST and PEC of 3-th microgrid are higher than operation separately, which represent that the benefit is damaged. Subgraphs (a), (b), and (c) in Figure 7 also show that the economic interests have been equilibrated best. Therefore, as shown in Table 5 and Figure 7, the proposed microgrids integrating V2G and V2B formulated multiobjective model can obtain multibenefits and achieve balance between global and individual benefits under a proeconomic weighting scenario.

5.3. Proenvironmental Scenario. In the proenvironmental scenario, $\omega_2 = 0.8$ and $\omega_1 = \omega_3 = 0.1$ are set to represent the proenvironmental attitude and adopt in the operation decision models. Table 6 displays the performances of each microgrid in microgrids, and the three models run for 311 seconds. In the reference model II under proenvironmental scenario, the centralized collective operation can achieve 22% CDE reduction and 12% PEC reduction when each microgrid's environmental pollution emission is reduced by different percentages. In order to balancing global and single benefit, model III is adopted to guarantee that each microgrid can have CDE reduction with same level. Based on the overall CDE reduction, β is set up to be 21% when there is no optimal

solution with average level (i.e., 22%). In addition, α as and δ are set be 0.

In Table 6, the values of f^I, f^{II}, and f^{III} under proenvironmental weighting scenario can be obtained with 0.67, 0.1586, and 0.338. Therefore, the multibenefits of the presented model III are inferior to reference II when ignoring individual benefits but also better than reference model I when considering microgrids running alone. Figure 8 shows that CDE reduction level of each microgrid in the proposed method is balanced than other models. As shown in Table 6 and Figure 8, although the benefits of microgrids reduced compared with neglecting interest balance, the proposed microgrids integrating V2G and V2B formulated multiobjective models can achieve balance between global and individual benefits under proenvironmental weighting scenario.

5.4. Proenergy Scenario. In the proenergy scenario, the reference models and model III are solved with $\omega_3 = 0.8$ and $\omega_1 = \omega_2 = 0.1$, which represents the proenergy attitude. Table 7 shows the performance of each microgrid in the microgrids, and the three models run for 322 seconds. In the reference model II under proenergy scenario, the centralized collective operation can achieve 12% CDE saving, 24% CDE reduction, and 9% PEC reduction, when each microgrid's PEC is reduced by a different percentage. Furthermore, Model III is adopted to guarantee that each microgrid can achieve PEC reduction at the same level. Based on the overall PEC reduction, δ is set up to be 8% when there is no optimal solution with average percentage (i.e., 9%). In addition, α and β are set be 0.

In Table 7, the values of f^I, f^{II}, and f^{III} under proenvironmental weighting scenario can be calculated with 1, 0, and 0.0017. Therefore, the multibenefits of formulated model III is similar with reference model II and better than reference I. The energy interest of each microgrid is achieved outstanding compared with reference models I and II (see Figure 9). As shown in Table 7 and Figure 9, the proposed microgrids integrating V2G and V2B formulated multiobjective model can achieve balance global and individual benefit under the proenergy weighting scenario, when the interest of microgrids basically guaranteed.

6. Conclusion

In this research, the multiobjective model is formulated to conduct a research on the transactive energy management for the microgrids integrating EVs. The COST, CDE, and PEC are selected as the economic, environmental, and energy indexes, respectively. Three different operation models are proposed to analyze the energy management in microgrids. The reference model I is formulated to maximize the total benefit with no exchange among microgrids. The reference model II is proposed to maximize collective interest under exchanging electricity and cooling energy among microgrids. The proposed model III is adopted to maximize collective interest within a satisfactory level of individual benefit. In the case study, microgrids located in Shanghai under different weighting scenarios are analyzed, and the mathematical models are solved by IBM's commercial solver CPLEX in Python with running average about 315 seconds. The experimental results indicate that proposed method can ensure benefit of each microgrid under weighting scenarios (i.e., decision maker's preference), when the multiple interest of microgrids is close to ignoring interest balance. For example, each microgrid have cost saving more than 6% under proeconomic weighting scenario. Therefore, the proposed method can be used to ensure the sustainable development for microgrids.

In this study, energy supply and demand are assumed as predetermined. However, they are influenced by many factors, such as extreme weather, equipment failure, and traffic congestion. In the future study, the energy management can be analyzed considering various uncertainties (e.g., solar radiation, energy load, and EV driving schedules). Robustness programming can be used in formulating stochastic optimization problems of microgrids. In addition, with the expansion of the scale of microgrids, the intelligent optimization algorithm can be adjusted and adopted to solve the microgrids' mathematical models.

Data Availability

The data used to support the findings of this study are available from the corresponding author upon request.

Conflicts of Interest

The authors declare that there are no conflicts of interest.

Authors' Contributions

Xiaolin Chu conceptualized the study, proposed the methodology, built the software, validated the study, and wrote the original draft. Peng Wang investigated the study, provided the software, and reviewed and edited the manuscript, and Dong Yang conceptualized the study, supervised the study, and reviewed and edited the manuscript.

Acknowledgments

This work was supported by the National Natural Science Foundation of China (No. 71971053); the 2022 Shanghai Teacher Professional Development Project and Training Program; the 2021 Golden Course of Shanghai Lixin University of Accounting and Finance; the 2022 Young Teacher Training Funding Program of Shanghai Universities; the Stable Operation Fund Project of the Key Laboratory of Electromagnetic Scattering (No. 622102Y070108); and the Shanghai Municipal Science and Technology Commission (No. 20ZR1454800).

References

[1] International Energy Agent, "World Energy Outlook 2021," 2021, https://iea.blob.core.windows.net/assets/4ed140c1-c3f3-4fd9-acae-789a4e14a23c/WorldEnergyOutlook2021.pdf.

[2] GenerlMicroGrids, "Microgrids: the self-healing solution," 2022, https://www.generalmicrogrids.com/about-us.
[3] A. H. Fathima and K. Palanisamy, "Optimization in microgrids with hybrid energy systems-a review," *Renewable and Sustainable Energy Reviews*, vol. 45, pp. 431–446, 2015.
[4] J. Tang, C. Yang, C. Feng, J. Li, X. Gu, and X. Jiang, "Energy cooperation optimization in residential microgrid with virtual storage technology," *Mathematical Problems in Engineering*, vol. 202111 pages, Article ID 8879122, 2021.
[5] G. Gust, T. Brandt, S. Mashayekh et al., "Strategies for microgrid operation under real-world conditions," *European Journal of Operational Research*, vol. 292, no. 1, pp. 339–352, 2021.
[6] R. H. Lasseter, "Microgrids and distributed generation," *Journal of Energy Engineering*, vol. 133, no. 3, pp. 144–149, 2007.
[7] R. H. Lasseter, "Smart distribution: coupled microgrids," *Proceedings of the IEEE*, vol. 99, no. 6, pp. 1074–1082, 2011.
[8] F. Moazeni and J. Khazaei, "Optimal operation of water-energy microgrids; a mixed integer linear programming formulation," *Journal of Cleaner Production*, vol. 275, Article ID 122776, 2020.
[9] S. Sukumar, H. Mokhlis, S. Mekhilef, K. Naidu, and M. Karimi, "Mix-mode energy management strategy and battery sizing for economic operation of grid-tied microgrid," *Energy*, vol. 118, pp. 1322–1333, 2017.
[10] Q. Jiang, M. Xue, and G. Geng, "Energy management of microgrid in grid-connected and stand-alone modes," *IEEE Transactions on Power Systems*, vol. 28, no. 3, pp. 3380–3389, 2013.
[11] T. Adefarati and R. C. Bansal, "Reliability, economic and environmental analysis of a microgrid system in the presence of renewable energy resources," *Applied Energy*, vol. 236, pp. 1089–1114, 2019.
[12] Z. Luo, Z. Wu, Z. Li, H. Y. Cai, B. J. Li, and W. Gu, "A two-stage optimization and control for CCHP microgrid energy management," *Applied Thermal Engineering*, vol. 125, pp. 513–522, 2017.
[13] Y. Li, Z. Yang, D. Zhao, H. Lei, B. Cui, and S. Li, "Incorporating energy storage and user experience in isolated microgrid dispatch using a multi-objective model," *IET Renewable Power Generation*, vol. 13, no. 6, pp. 973–981, 2019.
[14] S. Singh, S. Jagota, and M. Singh, "Energy management and voltage stabilization in an islanded microgrid through an electric vehicle charging station," *Sustainable Cities and Society*, vol. 41, pp. 679–694, 2018.
[15] M. H. Sarparandeh and M. Ehsan, "Pricing of vehicle-to-grid services in a microgrid by nash bargaining theory," *Mathematical Problems in Engineering*, vol. 2017, Article ID 1840140, 11 pages, 2017.
[16] X. Chu, Y. Ge, X. Zhou, L. Li, and D. Yang, "Modeling and analysis of electric vehicle-power-grid-manufacturing facility (EPM) energy sharing system under Time-of-Use electricity tariff," *Sustainability*, vol. 12, p. 4836, 2020.
[17] Y. Li, Z. Yang, G. Li et al., "Optimal scheduling of isolated microgrid with an electric vehicle battery swapping station in multi-stakeholder scenarios: a bi-level programming approach via real-time pricing," *Applied Energy*, vol. 232, pp. 54–68, 2018.
[18] Y. Li, M. Han, Z. Yang, and G. Li, "Coordinating flexible demand response and renewable uncertainties for scheduling of community integrated energy systems with an electric vehicle charging station: a bi-level approach," *IEEE Transactions on Sustainable Energy*, vol. 12, no. 4, pp. 2321–2331, 2021.
[19] B. Zhang, Q. Li, W. Feng, L. Wang, and W. Feng, "Robust optimization for energy transactions in multi-microgrids under uncertainty," *Applied Energy*, vol. 217, pp. 346–360, 2018.
[20] S. K. Rangu, P. R. Lolla, K. R. Dhenuvakonda, and A. R. Singh, "Recent trends in power management strategies for optimal operation of distributed energy resources in microgrids: a comprehensive review," *International Journal of Energy Research*, vol. 44, no. 13, pp. 9889–9911, 2020.
[21] C. Bahret, S. Köhler, L. Eltrop, and B. Schröter, "A case study on energy system optimization at neighborhood level based on simulated data: a building-specific approach," *Energy and Buildings*, vol. 238, Article ID 110785, 2021.
[22] A. Ouammi, H. Dagdougui, L. Dessaint, and R. Sacile, "Coordinated model predictive-based power flows control in a cooperative network of smart microgrids," *IEEE Transactions on Smart Grid*, vol. 6, no. 5, pp. 2233–2244, 2015.
[23] Y. Zhou, "Energy sharing and trading on a novel spatio-temporal energy network in Guangdong-Hong Kong-Macao Greater Bay Area," *Applied Energy*, vol. 318, Article ID 119131, 2022.
[24] Z. Wang, B. Chen, J. Wang, and J. Kim, "Decentralized energy management system for networked microgrids in grid-connected and islanded modes," *IEEE Transactions on Smart Grid*, vol. 7, no. 2, pp. 1097–1105, 2016.
[25] Q. Zhang, J. Ding, W. Shen, J. Ma, and G. Li, "Multiobjective particle swarm optimization for microgrids pareto optimization dispatch," *Mathematical Problems in Engineering*, vol. 202013 pages, Article ID 5695917, 2020.
[26] R. Jing, M. Wang, H. Liang et al., "Multi-objective optimization of a neighborhood-level urban energy network: considering Game-theory inspired multi-benefit allocation constraints," *Applied Energy*, vol. 231, pp. 534–548, 2018.
[27] Y. Du, Z. Wang, G. Liu et al., "A cooperative game approach for coordinating multi-microgrid operation within distribution systems," *Applied Energy*, vol. 222, pp. 383–395, 2018.
[28] Y. Chen and M. Hu, "Balancing collective and individual interests in transactive energy management of interconnected micro-grid clusters," *Energy*, vol. 109, pp. 1075–1085, 2016.
[29] M. Daneshvar, B. Mohammadi-Ivatloo, S. Asadi et al., "Chance-constrained models for transactive energy management of interconnected microgrids clusters," *Journal of Cleaner Production*, vol. 271, Article ID 122177, 2020.
[30] S. Nazila, B. Ezzeddin, H. Kasun, and S. Rehan, "Optimization of hydraulic fracturing wastewater management alternatives: a hybrid multi-objective linear programming model," *Journal of Cleaner Production*, vol. 286, Article ID 124950, 2021.
[31] R. Jing, M. Wang, N. Brandon, and Y. Zhao, "Multi-criteria evaluation of solid oxide fuel cell based combined cooling heating and power (SOFC-CCHP) applications for public buildings in China," *Energy*, vol. 141, pp. 273–289, 2017.
[32] J. L. Chen and G. S. Li, "Estimation of monthly average daily solar radiation from measured meteorological data in Yangtze River Basin in China," *International Journal of Climatology*, vol. 33, no. 2, pp. 487–498, 2013.
[33] Y. Kuang, Y. Chen, M. Hu, and D. Yang, "Influence analysis of driver behavior and building category on economic

performance of electric vehicle to grid and building integration," *Applied Energy*, vol. 207, pp. 427–437, 2017.

[34] R. Jing, X. Zhu, Z. Zhu et al., "A multi-objective optimization and multi-criteria evaluation integrated framework for distributed energy system optimal planning," *Energy Conversion and Management*, vol. 166, pp. 445–462, 2018.

[35] J. Wang, Y. Zhou, N. Lior, and G. Zhang, "Quantitative sustainability evaluations of hybrid combined cooling, heating, and power schemes integrated with solar technologies," *Energy*, vol. 231, p. 120783, 2021.